



Does integrated shimming improve lesion detection in whole-body diffusion-weighted examinations of patients with breast cancer?

Michiro Sasaki¹ · Mitsuhiro Tozaki² · Katsuya Maruyama³ · Thomas Benkert⁴ · Wakana Murakami⁵ · Daisuke Yotsumoto⁶ · Shunichi Oosako⁷ · Yoshiaki Sagara²

Received: 25 April 2018 / Accepted: 23 September 2018 / Published online: 27 September 2018
© Japan Radiological Society 2018

Abstract

Purpose To evaluate the feasibility of proposed integrated slice-by-slice shimming (iShim) for whole-body diffusion weighted imaging (WB-DWI) in comparison to conventional 3D shim in patients with breast cancer.

Materials and methods Retrospective analysis of 116 consecutive patients (116 lesions) who underwent whole-body PET/MR using iShim (iShim group) were performed and compared with historical control of 103 patients (105 lesions) using 3D Shim (3D Shim group).

Results As compared with dynamic contrast-enhanced (DCE) breast MRI, the apparent diffusion coefficient (ADC) value could not be determined for 15 (14%) of the 105 lesions of the 3D shim group and for 10 (9%) of the 116 lesions on iShim group. The intergroup difference failed to reach statistical significance ($P=0.1843$). On the other hand, there was a significant difference in the frequencies of PET-positive and DWI-negative lesions between the 3D shim and iShim group (8.6% vs. 1.7%, respectively, $P=0.01942$).

Conclusion In regard to detectability of breast cancers by DWI, iShim may allow improved detectability as compared to conventional 3D shim.

Keywords PET/MRI · Apparent diffusion coefficient · Diffusion-weighted imaging · Integrated slice-by-slice shimming · Breast carcinoma

✉ Michiro Sasaki
chacha622@sagara.or.jp

¹ Department of Radiology, Sagara Perth Avenue Clinic, 26-13 Shinyashiki-cho, Kagoshima city 892-0838, Kagoshima, Japan

² Department of Radiology, Sagara Hospital Affiliated Breast Center, 3-28 Tenokuchi-cho, Kagoshima city 892-0845, Kagoshima, Japan

³ MR Research & Collaboration Dpt. Diagnostic Imaging Business Area, Siemens Healthcare K.K, Erlangen, Germany

⁴ Siemens Healthcare GmbH, Erlangen, Germany

⁵ Department of Radiology, National Defense Medical College, 3-2 Namiki, Tokorozawa city, Saitama 359-0042, Japan

⁶ Department of Breast Surgery, Sagara Hospital, 3-31 Matsubara-cho, Kagoshima city 892-0833, Kagoshima, Japan

⁷ Image Inspection Department, Sagara Perth Avenue Clinic, 26-13 Shinyashiki-cho, Kagoshima city 892-0838, Kagoshima, Japan

Introduction

Conventional WB-DWI data based on 3D shimming usually lack homogeneity of the shimming data for the upper and lower parts of the body owing to the fact that shimming adjustment is to be done for each imaging separately. This leads, in particular, to occurrence of the broken spine phenomenon at the junction between neck and chest (lack of contiguity between the spine and spinal cord). In contrast, with iShim technique, homogeneous shimming data can be ensured by performing slice-by-slice shimming. For each subsequent imaging slice, the slice-specific shim data are applied. With this procedure, the broken spine phenomenon of the spinal cord in whole-body imaging is resolved and the homogeneity of signals from regions other than the spinal cord improves. Meanwhile, signal to noise ratio (SNR) decrease in the neck region has an impact on the ADC. It has been reported that, while there is no vital difference between 3D shim and iShim for imaging regions such as

the thoracoabdominal region and pelvic region, the precision of imaging in the neck region improves [1].

Echo-planar imaging (EPI) is sensitive to local off-resonance. Distortions Δd in EPI are proportional to the field of view in the phase-encoding direction (FOV_{PE}), the echo spacing Δt_{PE} , and the local off-resonance ΔB_0 : $\Delta d \approx FOV_{PE} \times \Delta t_{PE} \times \Delta B_0$. Recent technical developments in DWI acquisition, such as multishot (readout-segmented EPI) [2,3], parallel imaging, and zoomed techniques [4,5] have yielded less geometric distortion and higher image quality from the perspective of the reduced Δt_{PE} and FOV_{PE} . However, the aforementioned techniques are not clinically feasible for whole-body imaging because of the longer acquisition time, field of view (FOV) restrictions, and sensitivity to motion. In addition to the aforementioned methods, another approach is to optimize the B_0 homogeneity [1]. The iShim technique is designed to reduce the local off-resonance term, B_0 . A recent study using slice-dependent shimming has also shown improved image quality in 3 T breast DWI [6]. However, its advantage for WB-DWI is still unknown.

In our previous reported work [7], we encountered cases with difficulty in visual assessment of the WB-DWI in patients in the supine position, as compared to DWI in patients in the prone position. Therefore, it was assumed that application of the iShim technique, which has been shown to improve the signal integrity and spatial alignment, might lead to improved breast cancer-detection performance.

The purpose of this study was to evaluate the feasibility of the proposed iShim technique for WB-DWI in comparison to conventional 3D shim-based shimming adjustment for each thoracic area in patients with breast cancer, in terms of the detection sensitivity.

Materials and methods

Patients

This retrospective study was conducted with the approval of our institutional review board. All the patients provided written informed consent for our review of their medical records and images.

In the present study, pertinent data on patients who had undergone PET/MRI scans for preoperative evaluations were collected retrospectively from the image database at this institution. All patients were diagnosed as having breast cancer by histopathology and treated by surgery.

Between May 2017 and July 2017, whole-body PET/MRI with the patients in the supine position and breast PET/MRI with the patients in the prone position were performed for pre-operative evaluations in 103 consecutive patients (age range 31–83 years; median 58 years) with a total of 105

breast cancers, using the conventional 3D shim (referred to as “3D shim group” in the following).

Between August 2017 and November 2017, whole-body PET/MRI with the patients in the supine position and breast PET/MRI with the patients in the prone position were performed for pre-operative evaluations in 116 consecutive patients with a total of 116 breast cancers (age range 34–84 years; median 60 years) at our hospital, using the iShim (referred to as “iShim group” in the following).

Imaging protocol

Patients fasted for at least 4–6 h before the intravenous administration of 18F-FDG with average radioactivity of 185MBq (3.7 MBq/kg of body weight).

First, a supine whole-body PET/MR scan was performed 60–100 min after the injection of 18F-FDG, covering a field of view from the parietal region to the mid thighs. After whole-body PET/MR was completed in the supine position, breast PET/MRI was performed with the patients in the prone position; the scan was started approximately 90–130 min after the injection.

The integrated PET/MR scanner (Biograph mMR; Siemens Healthcare GmbH, Erlangen, Germany) consists of a 3-T MR system and PET system with an avalanche photodiodes (APD) detector. The APD are relatively insensitive to a magnetic field and are located in the MR gantry between the RF body coil and the gradient coils. The PET unit has an axial field of view of 25.8 cm resulting in 4–5 bed positions depending on the patient’s height. The PET data were acquired for 4 min per bed position and reconstructed using a three-dimensional (3D) Ordinary Poisson Ordered-Subsets Expectation Maximization with point spread function algorithm with 3 iterations and 21 subsets (172×172 matrix, zoom 1, slice thickness 2 mm). A post-reconstruction Gaussian filter with 4.0 mm full-width at half maximum was applied. An MRI-based attenuation correction of the PET data was accomplished according to the method described by Martinez-Moller et al. [8]. The imaging protocol was designed with reference to the study by Martinez-Moller et al. [9].

Whole-body PET/MR was performed in a caudocranial direction using total imaging matrix (Tim) phased array coils. After acquisition of the initial T1-weighted two-point Dixon 3D volumetric interpolated breath-hold examination (VIBE) for attenuation correction, axial T1-weighted VIBE, axial T2-weighted half-Fourier single-shot turbo spin-echo (HASTE) sequences and axial diffusion weighted imaging (DWI; $b = 0$, $b = 800$) were obtained during simultaneous PET acquisition.

The breast PET/MRI comprised a breast PET scan of 1 bed position and a simultaneous breast MRI using a standard 4-channel breast coil. The emission time of the PET

scan was 15 min. The breast MRI examination consisted of a localizer sequence, coronal T1-weighted turbo spin-echo, and sagittal T2-weighted fat-suppressed turbo spin-echo sequence, coronal a single-shot echo planar diffusion-weighted sequence (DWI; $b=0$, $b=1000$), and 3D dynamic contrast-enhanced (DCE) sequence. DCE-MRI was performed with coronal T1-weighted fat-suppressed 3D VIBE, with 1 pre-contrast and 3 post-contrast dynamic series performed within 5 min depending on the breast thickness after bolus injection. Next, 1 mL/s of gadobutrol (0.1 mmol/kg of body weight, Gadovist; Bayer Schering Pharma, Berlin, Germany) was injected, followed by a 20-mL saline flush.

Shimming techniques

In the conventional 3D shim protocol, high-order shim (up to second order) was applied and single-center frequency was determined for the entire stack of slices in each bed position.

In the iShim protocol, the above-mentioned conventional 3D shim was disabled. The acquisition of the field map was integrated into a prototypical single-shot DWI EPI sequence (iShim). During the initial calibration phase, 2D dual-echo FLASH (Fast Low-Angle SHot) images were acquired which were used to calculate slice-specific field maps. For the

resulting, stack of field map slices, a center frequency and linear shim terms were calculated individually for each slice. During the imaging phase, the frequency and the linear shim terms were then dynamically updated prior to the acquisition of each slice [1] (Fig. 1). The time for the acquisition of the field map was approximately 700 ms per slice, resulting in 21 s for a 30-slice station. The imaging parameters are listed in detail in Table 1.

Whole body PET/MRI

The DWI and PET images were evaluated visually and quantitatively by one experienced radiologist (M.S) with 25 years of experience with knowledge of the clinical information and the presence of breast carcinoma. Then the radiologist tried to measure the ADC for the respective lesion. The ADC value was calculated according to the formula: $ADC = [1/(b_2 - b_1)] \ln(S_1/S_2)$, where S_1 and S_2 are the signal intensities in the ROI obtained by two gradient factors, b_2 and b_1 ($b_1 = 0$ and $b_2 = 800 \text{ s/mm}^2$). For the measurement of the ADC value, one radiologist (M.S) placed a region of interest (ROI) within the tumor on the ADC map by referring to the solid portion of DCE, T1WI, T2WI and fusion imaging, according to the methods published previously [10]. The

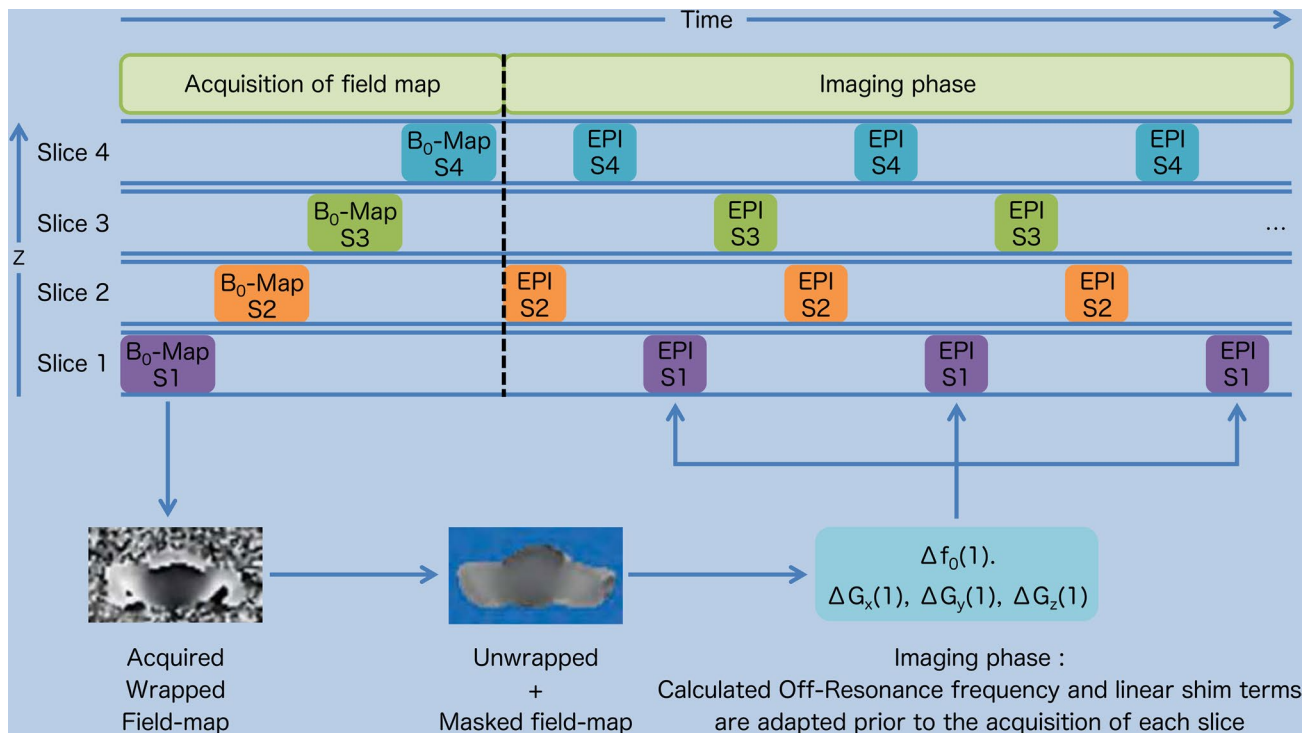


Fig. 1 Schematics of the prototypical iShim sequence. The acquisition of the field map was integrated into the single-shot DWI EPI sequence. During the initial calibration phase, 2D dual-echo FLASH (Fast Low-Angle SHot) images were acquired which were used to calculate slice-specific field maps. For the resulting stack of field map

slices, a center frequency and linear shim terms were calculated individually for each slice. During the imaging phase the frequency and the linear shim terms are then dynamically updated prior to the acquisition of each slice

Table 1 Sequence parameters of WBMRI protocol

Parameter	iShim WBDWI	3D shim
Scan plane	Transversal	
Acquisition dimension	2D	
Scan period	August 2017 and November 2017 (<i>N</i> = 116)	May 2017 and July 2017 (<i>N</i> = 105)
Acceleration	GRAPPA, 2	
No. slices per station	30	
Slice thickness, mm	6.5	
Gap between slices, mm	0	
In-plane FOV, mm	450 × 425	450 × 393.8
Plane resolution, mm	4.17 × 4.17	3.52 × 3.52
No. stations/bed positions	5–6 (depending on height to cover from head to thigh)	5–6 (depending on height to cover from head to thigh)
TR/TE, ms	4650/55	4830/50
Fat suppression	Slice-selective inversion recovery	STIR
<i>b</i> , s/mm ²	0, 800	
Acquisition time per station, s	111	136

ROIs were carefully placed inside the tumor avoiding the cystic portion or any visual artifact, and the mean ADC values within each ROI were recorded. We calculated the average of the mean ADC values for all ROIs within the tumor. For quantitative analysis of FDG uptake, a volume of interest (VOI) was placed over the most intense area of FDG accumulation by the primary breast tumor for each patient. PET scans with focally marked increased FDG uptake were considered definite. Moreover, the cases with diffuse or slightly to moderate focally increased FDG uptake were considered positive to represent malignant tissue. The SUV was calculated as: $SUV = VOI \text{ radioactivity concentration (Bq/mL)} / [\text{injected dose (Bq)} / \text{patient's weight (g)}]$. SUV_{max}, which was defined as the highest SUV in the pixel with the highest count within the VOI, was measured and recorded for the focal areas of uptake.

Breast PET/MRI as the reference standard

For the DCE-MRI analysis, subtraction images were generated by subtracting the pre-contrast images from all contrast-enhanced images. Subsequently, the tumor size, morphologic pattern (shape, margin, and internal enhancement of the mass lesion) during the early phase, and kinetics (percentage signal intensity increase during the early phase and kinetic curve type during the delayed phase) were evaluated for each lesion according to the Breast Imaging Reporting and Data System MRI guidelines [11].

Statistical analysis

The statistical analyses were performed with the R statistical software, version (3.2.3) [3]. A *p* value of <0.05 was

considered to be indicative of statistical significance. In the analysis of the diagnostic performance of both the iShim and 3D shim DWI sequences, the number of detected suspicious lesions using DWI and PET was evaluated for each of the DWI techniques and then compared using the χ^2 test and Z test. In addition, the relationships between 3D Shim group, iShim group, and the clinical situations (age, size and histopathological situations) were calculated using the Mann–Whitney *U* test and the χ^2 test (for two groups).

We examined whether there was a difference in the detection capability for breast cancer between the 103 cases that underwent PET/MRI and DWI using the conventional 3D shim and the 116 cases who underwent imaging with iShim.

Results

All breast cancers could be detected on DCE-MRI.

Histopathology

3D shim group with a malignant biopsy result underwent a mastectomy or breast-conserving surgery. The histologic types of malignancy included ductal carcinoma in situ (DCIS) (*n* = 14), invasive ductal carcinoma, not otherwise specified (ductal NOS) (*n* = 83, including papillotubular carcinoma in 17, solid-tubular carcinoma in 23, and scirrhous carcinoma in 43), invasive lobular carcinoma (*n* = 5), and mucinous carcinoma (*n* = 3). The average size of the invasive tumors was 36.7 mm (range 4.0–115.0 mm), while that of the DCIS lesions was 33.7 mm (range 4.0–80.0 mm). When classified according to the histological grade, 45 tumors were nuclear grade 1, and 46 tumors were grade 2 or 3.

Meanwhile, iShim group with a malignant biopsy result underwent a mastectomy or breast-conserving surgery between August 2017 and November 2017. The histologic types of malignancy included ductal carcinoma in situ (DCIS) ($n = 15$), invasive ductal carcinoma, not otherwise specified (ductal NOS) ($n = 88$, including papillotubular carcinoma in 24, solid-tubular carcinoma in 19, and scirrhous carcinoma in 45), invasive lobular carcinoma ($n = 7$), mucinous carcinoma ($n = 3$), adenoid cystic carcinoma ($n = 1$), and apocrine carcinoma ($n = 2$). The average size of the invasive tumors was 17.1 mm (range 1.0–80 mm), while that of the DCIS lesions was 34.4 mm (range, 4.0–90 mm). When classified according to the histological grade, 56 tumors were nuclear grade 1, and 49 tumors were grade 2 or 3.

There was no difference in the clinical situation between the 3D shim group and the iShim group (Table 2).

Visual assessment of DWI

Of the 105 lesions which were found by dynamic MRI in the 3D shim group, it was not feasible to determine the apparent diffusion coefficient (ADC) value in whole body PET/MRI for 15 lesions (14%) because of the likelihood of artifacts and coil sensitivity unevenness in the step border due to respiratory movements, as summarized in Table 3. Similarly, there were 10 lesions (9%) among the 116 lesions in the iShim group, for which the ADC value could not be determined. While the percentage was decreased, there was no statistically significant difference in the incidence of failure of lesion detection ($P = 0.1843$) between the two groups.

As can be seen in Table 4, among undetectable lesions in the 3D shim group, the standardized uptake value (SUV) value was measurable, whereas the ADC value was

Table 2 Association in the clinical situation between 3D shim and iShim group

	Whole body (3D Shim), $N = 105$	Whole body (iShim), $N = 105$	P value
Age, y/o			
Median	60	61	0.5862
Range	31–83	34–84	
Extent (IDC), mm			
Median	30	27.5	0.1983
Range	4–115	5–105	
Extent (DCIS), mm			
Median	35	20	0.9338
Range			
Histological grade			
I	45	56	0.6898
II, III	46	49	

IDC invasive ductal carcinoma, DCIS ductal carcinoma in situ

Table 3 Visual assessment of diffusion-weighted imaging and PET imaging

	Whole body (3D Shim), $N = 105$		Whole body (iShim), $N = 116$	
	Negative	Positive	Negative	Positive
DWI	15	90	10	106
PET	6	99	8	108

unmeasurable for 9 (8.6%) of the 105 lesions. In the iShim group, the SUV value alone was measurable and the ADC value was unmeasurable for 2 (1.7%) of the 116 lesions. Thus, there was a significant reduction in the incidence of failure to determine the ADC value in the iShim group ($P = 0.01942$). Both the SUV and the ADC value were unmeasurable for 6 (5.7%) of the 105 lesions in the 3D shim group and for 8 (6.9%) of the 116 lesions in the iShim group; hence, no significant intergroup difference was noted in this respect ($P = 0.7186$). Figures 2 and 3 show representative data from the 3D shim cases and iShim cases, respectively.

Discussion

The improvement of shimming data and signal uniformity is very important in MRI images.

Improvements in DWI, which is a more non-invasive tool than DCE-MRI, are of profound significance to patients. Moreover, this tool is expected to play an important role, not merely in improving breast cancer detection rates, but also in evaluating distant metastases. The present study has been designed to explore whether breast cancer detection could be improved by adopting the iShim technique. The intergroup difference failed to reach statistical significance, but improvement of the sensitivity of lesion detection was evident with iShim ($P = 0.1843$). However, there was a significant reduction in the incidence of failure to determine the ADC, while the SUV alone was measurable in the iShim group ($P = 0.01942$). With the iShim technique, the number of lesions that could not be identified on WB-DWI decreased, and the breast lesions visualized by PET

Table 4 Visual assessment of diffusion-weighted imaging and PET imaging

	Whole body (3D Shim), negative $N = 105$	Whole body (iShim), negative $N = 116$	$p = 0.01942$
D(−) and P(+)	9	2	
D(−) and P(−)	6	8	

D(−) not depiction on DWI, P(+) depiction on PET imaging, P(−) not depiction on PET imaging

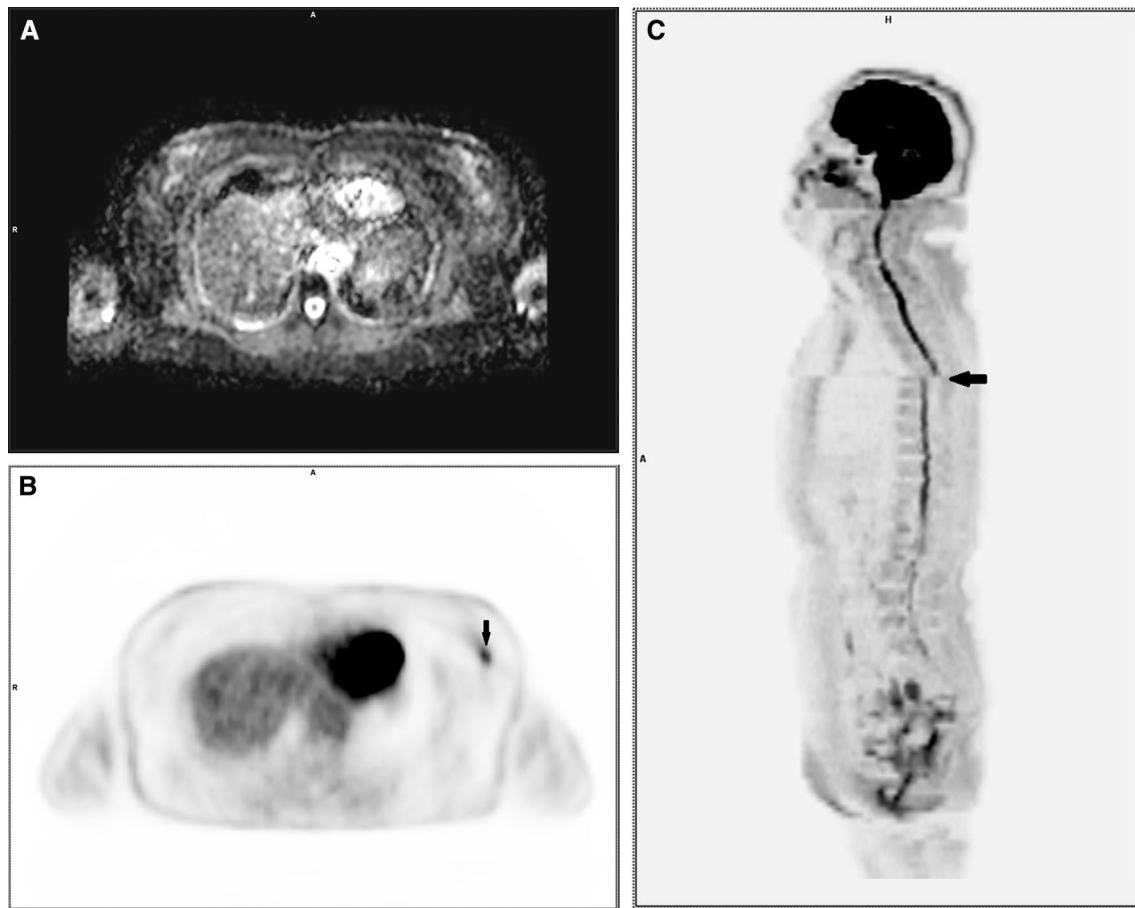


Fig. 2 Whole-body PET/MR images using the 3D shim of 61-year-old patient with invasive ductal carcinoma of the left breast. **a** Gray scale axial ADC map could not depict the left breast tumor. **b** PET images show that the lesion is associated to a focal uptake of ^{18}F -

FDG (arrow). **c** A sagittal reformats of WB-DWI images acquired using the 3D shim show the signal discontinuity across adjacent bed positions (arrow). **c**

became detectable even on DWI. Thus, the frequency of breast cancer detection with the use of the iShim technique is considered to be equal to or even better than that with the conventional WB-DWI (3D shim WB-DWI).

Paucity of the SNR changes in the thoracic region including the breast might account, at least in part, for the failure in achieving a statistically significant intergroup difference in the detection sensitivity, even though it has been reported that there were no appreciable SNR changes in other regions than the neck with iShim as compared to 3D Shim [1].

Our present study had several limitations. First, there is the slight discrepancy of different imaging parameters (Table 1, e.g., resolution, acquisition time, TR). Second, the relatively small sample sizes seemed to account for the failure to obtain a statistically significant intergroup difference in the sensitivity of lesion detection, although the data imply improvement of this parameter on DWI using

iShim as compared to 3D shim. Third, 3D Shim group and iShim group were different, not same patients and not same lesions. Fourth, one radiologist took charge of the ADC measurement throughout this study, which potentially entails the problem of ADC data reproducibility. Fifth, the present investigation was not a double-blinded prospective study, but a retrospective study, with interpretation of the images carried out by investigators with knowledge about other relevant imaging data and clinical information. This likely introduced some bias.

In conclusion, the improvement of shimming data and signal uniformity using iShim is very important in MRI images, so the ADC is more reliable with iShim. Compared with conventional 3D shim, the number of lesions on DWI was matched equally or better when iShim was used. Further investigation of 3D shim versus iShim with greater precision in accumulated clinical cases is warranted.

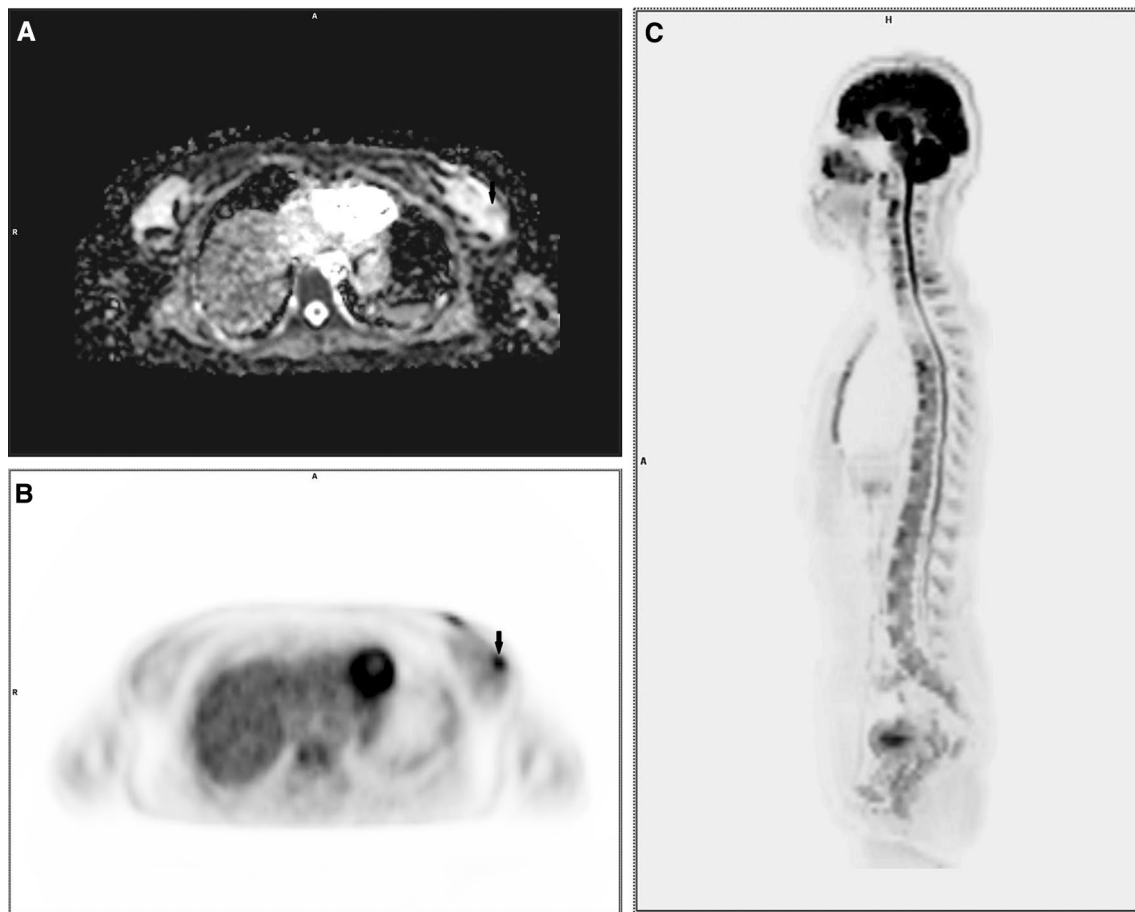


Fig. 3 Whole-body PET/MR images of 40-year-old patient with invasive ductal carcinoma of the left breast using the iShim technique. **a** Gray scale axial ADC map could depict the left breast tumor (arrow). **b** PET images show that the lesion is associated to a focal uptake

of ^{18}F -FDG (arrow). The iShim parameters successfully corrected the signal discontinuity across adjacent bed positions, which was observed with conventional 3D shim (**c**)

Compliance with ethical standards

Conflict of interest Thomas Benkert and Katsuya Maruyama are employees of Siemens Healthcare, who provided crucial technical support with the MR sequence but were not involved in data acquisition and analysis. The authors declare that they have no conflict of interest.

Ethical approval This retrospective study was conducted with the approval of our institutional review board. All the patients provided written informed consent for our review of their medical records and images.

References

- Zhang H, Xue H, Alto S, Hui L, Kannengiesser S, Berthold K, et al. Integrated shimming improves lesion detection in whole-body diffusion-weighted examinations of patients with plasma disorder at 3 T. *Invest Radiol*. 2016;51(5):297–305.
- Bogner W, Pinker-Domenig K, Bickel H, Chmelik M, Weber M, Helbich TH, et al. Readout-segmented echo-planar imaging improves the diagnostic performance of diffusion-weighted MR breast examinations at 3.0 T. *Radiology*. 2012;263(1):64–76.
- Chen N, Guidon A, Chang HC, Song AW. A robust multi-shot scan strategy for high-resolution diffusion weighted MRI enabled by multiplexed sensitivity-encoding (MUSE). *Neuroimage*. 2013;72(9):41–7.
- Riffel P, Michaely HJ, Morelli JN, Pfeuffer J, Attenberger UI, Schoenberg SO, et al. Zoomed EPI-DWI of the head and neck with two-dimensional, spatially-selective radiofrequency excitation pulses. *Eur Radiol*. 2014;24(10):2507–12.
- Thierfelder KM, Scherr MK, Notohamiprodjo M, Weiß J, Dietrich O, Mueller-Lisse UG, et al. Diffusion-weighted MRI of the prostate: advantages of zoomed EPI with parallel-transmit-accelerated 2D-selective excitation imaging. *Eur Radiol*. 2014;24(12):3233–41.
- Lee SK, Tan ET, Govanar A, Hancu I. Dynamic slice-dependent shim and center frequency update in 3 T breast diffusion weighted imaging. *Magn Reson Med*. 2014;71(5):1813–8.
- Sasaki M, Tozaki M, Kubota K, Murakami W, Yotsumoto D, Sagara Y, et al. Simultaneous whole-body and breast ^{18}F -FDG PET/MRI examinations in patients with breast cancer: a comparison of apparent diffusion coefficients and maximum standardized uptake values. *Jpn J Radiol*. 2018;36(2):122–33.

8. Martinez-Moller A, Souvatzoglou M, Delso G, Bundschuh RA, Ched'hotel C, Ziegler SI, et al. Tissue classification as a potential approach for attenuation correction in whole-body PET/MRI: evaluation with PET/CT data. *J Nucl Med.* 2009;50(4):520–6.
9. Martinez-Moller A, Eiber M, Nekolla SG, Souvatzoglou M, Drzezga A, Ziegler S, et al. Workflow and scan protocol considerations for integrated whole-body PET/MRI in oncology. *J Nucl Med.* 2012;53(9):1415–26.
10. Choi BB, Kim SH, Kang BJ, Lee JH, Song BJ, Jeong SH, et al. Diffusion-weighted imaging and FDG PET/CT: predicting the prognoses with apparent diffusion coefficient values and maximum standardized uptake values in patients with invasive ductal carcinoma. *World J Surg Oncol.* 2012;10(9):126.
11. American College of Radiology. Breast imaging reporting and data system: breast imaging atlas (BI-RADS). 5th ed. Reston Va: ACR; 2013.
12. Kanda Y. Investigation of the freely available easy-to-use software 'EZR' for medical statistics. *Bone Marrow Transpl.* 2013;48(3):452–8.